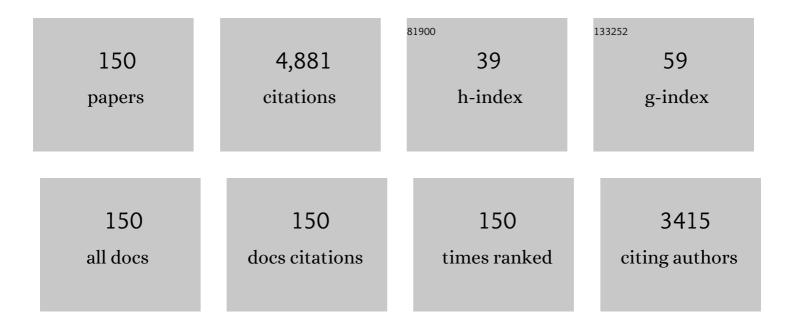
List of Publications by Year in descending order

Source: https://exaly.com/author-pdf/4927519/publications.pdf Version: 2024-02-01



#	Article	IF	CITATIONS
1	An Ordered Mesoporous Aluminosilicate with Completely Crystalline Zeolite Wall Structure. Journal of the American Chemical Society, 2006, 128, 10636-10637.	13.7	206
2	Effect of inorganic matter on reactivity and kinetics of coal pyrolysis. Fuel, 2004, 83, 713-718.	6.4	190
3	Analysis of coal tar derived from pyrolysis at different atmospheres. Fuel, 2013, 104, 14-21.	6.4	156
4	Hierarchical porous carbons prepared from direct coal liquefaction residue and coal for supercapacitor electrodes. Carbon, 2013, 55, 221-232.	10.3	134
5	Hydrogen production by catalytic methane decomposition: Carbon materials as catalysts or catalyst supports. International Journal of Hydrogen Energy, 2017, 42, 19755-19775.	7.1	125
6	Nonisothermal Catalytic Liquefaction of Corn Stalk in Subcritical and Supercritical Water. Energy & Fuels, 2004, 18, 90-96.	5.1	109
7	Pyrolysis behavior of vitrinite and inertinite from Chinese Pingshuo coal by TG–MS and in a fixed bed reactor. Fuel Processing Technology, 2011, 92, 780-786.	7.2	106
8	Product distribution and sulfur behavior in coal pyrolysis. Fuel Processing Technology, 2004, 85, 849-861.	7.2	98
9	In-situ catalytic upgrading of coal pyrolysis tar on carbon-based catalyst in a fixed-bed reactor. Fuel Processing Technology, 2016, 147, 41-46.	7.2	85
10	In Situ Assembly of Zeolite Nanocrystals into Mesoporous Aggregate with Single-Crystal-Like Morphology without Secondary Template. Chemistry of Materials, 2008, 20, 1670-1672.	6.7	76
11	In situ FT-IR spectroscopic studies on thermal decomposition of the weak covalent bonds of brown coal. Journal of Analytical and Applied Pyrolysis, 2015, 115, 262-267.	5.5	73
12	Pyrolysis Behaviors of Tumuji Oil Sand by Thermogravimetry (TG) and in a Fixed Bed Reactor. Energy & Fuels, 2007, 21, 2245-2249.	5.1	69
13	Preparation of activated carbon supported Fe–Al2O3 catalyst and its application for hydrogen production by catalytic methane decomposition. International Journal of Hydrogen Energy, 2013, 38, 10373-10380.	7.1	68
14	Integrated coal pyrolysis with CO2 reforming of methane over Ni/MgO catalyst for improving tar yield. Fuel Processing Technology, 2010, 91, 419-423.	7.2	67
15	Role of Iron-Based Catalyst and Hydrogen Transfer in Direct Coal Liquefaction. Energy & Fuels, 2008, 22, 1126-1129.	5.1	65
16	Effect of inherent and additional pyrite on the pyrolysis behavior of oil shale. Journal of Analytical and Applied Pyrolysis, 2014, 105, 342-347.	5.5	65
17	Preparation of Ni/MgO catalyst for CO2 reforming of methane by dielectric-barrier discharge plasma. Catalysis Communications, 2010, 11, 968-972.	3.3	64
18	Effect of Atmosphere on Evolution of Sulfur-Containing Gases during Coal Pyrolysis. Energy & Fuels, 2005, 19, 892-897.	5.1	63

#	Article	IF	CITATIONS
19	A review on high catalytic efficiency of solid acid catalysts for lignin valorization. Bioresource Technology, 2020, 298, 122432.	9.6	63
20	Effect of temperature and simulated coal gas composition on tar production during pyrolysis of a subbituminous coal. Fuel, 2019, 241, 1129-1137.	6.4	60
21	Mesoporous carbon prepared from direct coal liquefaction residue for methane decomposition. Carbon, 2012, 50, 952-959.	10.3	54
22	A theoretical study on bond dissociation enthalpies of coal based model compounds. Fuel, 2015, 153, 70-77.	6.4	54
23	Approach for promoting liquid yield in direct liquefaction of Shenhua coal. Fuel Processing Technology, 2008, 89, 1090-1095.	7.2	53
24	Effect of tetrahydrofuran extraction on lignite pyrolysis under nitrogen. Journal of Analytical and Applied Pyrolysis, 2015, 112, 113-120.	5.5	53
25	Pyrolysis of Huolinhe lignite extract by in-situ pyrolysis-time of flight mass spectrometry. Fuel Processing Technology, 2015, 135, 52-59.	7.2	52
26	Integrated coal pyrolysis with methane aromatization over Mo/HZSM-5 for improving tar yield. Fuel, 2013, 114, 187-190.	6.4	51
27	Fast co-pyrolysis of a massive Naomaohu coal and cedar mixture using rapid infrared heating. Energy Conversion and Management, 2020, 205, 112442.	9.2	50
28	CO2 reforming of methane on Ni/γ-Al2O3 catalyst prepared by dielectric barrier discharge hydrogen plasma. International Journal of Hydrogen Energy, 2014, 39, 5756-5763.	7.1	49
29	Direct liquefaction behaviors of Bulianta coal and its macerals. Fuel Processing Technology, 2014, 128, 232-237.	7.2	46
30	Effect of functional groups on volatile evolution in coal pyrolysis process with in-situ pyrolysis photoionization time-of-flight mass spectrometry. Fuel, 2020, 260, 116322.	6.4	46
31	Pyrolysis Behavior of Weakly Reductive Coals from Northwest China. Energy & Fuels, 2009, 23, 870-875.	5.1	44
32	Pyrolysis behaviors of two coal-related model compounds on a fixed-bed reactor. Fuel Processing Technology, 2015, 129, 113-119.	7.2	44
33	Ni doped carbons for hydrogen production by catalytic methane decomposition. International Journal of Hydrogen Energy, 2013, 38, 3937-3947.	7.1	43
34	Effect of reducibility of transition metal oxides on in-situ oxidative catalytic cracking of tar. Energy Conversion and Management, 2019, 197, 111871.	9.2	43
35	Preparation of Fe-Doped Carbon Catalyst for Methane Decomposition to Hydrogen. Industrial & Engineering Chemistry Research, 2017, 56, 11021-11027.	3.7	42
36	Effect of hydrothermal treatment on structure and liquefaction behavior of Baiyinhua coal. Fuel Processing Technology, 2017, 167, 648-654.	7.2	42

#	Article	IF	CITATIONS
37	Effect of mineral in coal on preparation of activated carbon for methane decomposition to hydrogen. Fuel, 2019, 258, 116138.	6.4	42
38	Insight into the aromatic ring structures of a low-rank coal by step-wise oxidation degradation. Fuel Processing Technology, 2020, 210, 106563.	7.2	42
39	Catalytic hydrogenolysis of lignin β-O-4 aryl ether compound and lignin to aromatics over Rh/Nb2O5 under low H2 pressure. Fuel Processing Technology, 2020, 203, 106392.	7.2	42
40	Synthesis of 2,6-dimethylnaphthalene by methylation of 2-methylnaphthalene on mesoporous ZSM-5 by desilication. Catalysis Communications, 2008, 10, 336-340.	3.3	41
41	Hierarchical porous carbon catalyst for simultaneous preparation of hydrogen and fibrous carbon by catalytic methane decomposition. International Journal of Hydrogen Energy, 2013, 38, 8732-8740.	7.1	41
42	Experimental and Theoretical Study on the Pyrolysis Mechanism of Three Coal-Based Model Compounds. Energy & Fuels, 2014, 28, 980-986.	5.1	41
43	Selective synthesis of 2,6-dimethylnaphthalene by methylation of 2-methylnaphthalene with methanol on Zr/(Al)ZSM-5. Catalysis Communications, 2006, 7, 255-259.	3.3	40
44	Catalytic upgrading of lignite pyrolysis volatiles over modified HY zeolites. Fuel, 2020, 259, 116234.	6.4	40
45	Effect of Fe components in red mud on catalytic pyrolysis of low rank coal. Journal of the Energy Institute, 2022, 100, 1-9.	5.3	40
46	Hydrogen peroxide oxidation degradation of a low-rank Naomaohu coal. Fuel Processing Technology, 2020, 207, 106484.	7.2	36
47	Isotope Analysis for Understanding the Tar Formation in the Integrated Process of Coal Pyrolysis with CO ₂ Reforming of Methane. Energy & Fuels, 2010, 24, 4402-4407.	5.1	35
48	Distribution of hydroxyl group in coal structure: A theoretical investigation. Fuel, 2017, 189, 195-202.	6.4	35
49	Desulfurization of Coal by Pyrolysis and Hydropyrolysis with Addition of KOH/NaOH. Energy & Fuels, 2005, 19, 1673-1678.	5.1	34
50	In Situ Analysis of Catalytic Effect of Calcium Nitrate on Shenmu Coal Pyrolysis with Pyrolysis Vacuum Ultraviolet Photoionization Mass Spectrometry. Energy & Fuels, 2018, 32, 1061-1069.	5.1	34
51	Lignin Valorizations with Ni Catalysts for Renewable Chemicals and Fuels Productions. Catalysts, 2019, 9, 488.	3.5	34
52	Kinetics of coal liquefaction during heating-up and isothermal stages. Fuel, 2008, 87, 508-513.	6.4	33
53	Catalytic methane decomposition over activated carbons prepared from direct coal liquefaction residue by KOH activation with addition of SiO 2 or SBA-15. International Journal of Hydrogen Energy, 2011, 36, 8978-8984.	7.1	33
54	Preparation and applications of hierarchical porous carbons from direct coal liquefaction residue. Fuel, 2013, 109, 2-8.	6.4	32

#	Article	IF	CITATIONS
55	Partial oxidation of vacuum residue over Al and Zr-doped α-Fe2O3 catalysts. Fuel, 2017, 210, 803-810.	6.4	32
56	In-situ catalytic upgrading of coal pyrolysis tar coupled with CO2 reforming of methane over Ni-based catalysts. Fuel Processing Technology, 2018, 177, 119-128.	7.2	32
57	Effect of different acid-leached USY zeolites on in-situ catalytic upgrading of lignite tar. Fuel, 2020, 266, 117089.	6.4	32
58	Controllable synthesis of chainlike hierarchical ZSM-5 templated by sucrose and its catalytic performance. Catalysis Communications, 2016, 75, 32-36.	3.3	31
59	Effect of Ca(NO3)2 addition in coal on properties of activated carbon for methane decomposition to hydrogen. Fuel Processing Technology, 2018, 176, 85-90.	7.2	31
60	Integrated Process of Coal Pyrolysis with Steam Reforming of Methane for Improving the Tar Yield. Energy & Fuels, 2014, 28, 7377-7384.	5.1	30
61	Effect of hydrogen additive on methane decomposition to hydrogen and carbon over activated carbon catalyst. International Journal of Hydrogen Energy, 2018, 43, 17611-17619.	7.1	28
62	Integrated process for partial oxidation of heavy oil and in-situ reduction of red mud. Applied Catalysis B: Environmental, 2019, 258, 117944.	20.2	28
63	In-situ catalytic upgrading of coal pyrolysis tar over activated carbon supported nickel in CO2 reforming of methane. Fuel, 2019, 250, 203-210.	6.4	28
64	Upgrading of vacuum residue with chemical looping partial oxidation over Ce doped Fe2O3. Energy, 2018, 162, 542-553.	8.8	27
65	Pyrolytic behavior of coal-related model compounds connected with C–C bridged linkages by in-situ pyrolysis vacuum ultraviolet photoionization mass spectrometry. Fuel, 2019, 241, 533-541.	6.4	27
66	Pyrolysis Behavior of Macerals from Weakly Reductive Coals. Energy & Fuels, 2010, 24, 6314-6320.	5.1	26
67	lsotope analysis for understanding the hydrogen transfer mechanism in direct liquefaction of Bulianta coal. Fuel, 2017, 203, 82-89.	6.4	26
68	In-situ analysis of catalytic pyrolysis of Baiyinhua coal with pyrolysis time-of-flight mass spectrometry. Fuel, 2018, 227, 386-393.	6.4	26
69	Effect of air pre-oxidization on coal-based activated carbon for methane decomposition to hydrogen. International Journal of Hydrogen Energy, 2016, 41, 10661-10669.	7.1	25
70	Preparation of carbon-Ni/MgO-Al2O3 composite catalysts for CO2 reforming of methane. International Journal of Hydrogen Energy, 2017, 42, 5047-5055.	7.1	25
71	Ni/MgO Al2O3 catalyst derived from modified [Ni,Mg,Al]-LDH with NaOH for CO2 reforming of methane. International Journal of Hydrogen Energy, 2018, 43, 2689-2698.	7.1	25
72	Fast pyrolysis behaviors of cedar in an infrared-heated fixed-bed reactor. Bioresource Technology, 2019, 290, 121739.	9.6	25

#	Article	IF	CITATIONS
73	<i>In Situ</i> Catalytic Upgrading of Coal Pyrolysis Tar over Carbon-Based Catalysts Coupled with CO ₂ Reforming of Methane. Energy & Fuels, 2017, 31, 9356-9362.	5.1	24
74	Upgrading of vacuum residue with chemical looping partial oxidation over Fe-Mn mixed metal oxides. Fuel, 2019, 239, 764-773.	6.4	24
75	Catalytic cracking of coal-tar model compounds over ZrO2/Al2O3 and Ni-Ce/Al2O3 catalysts under steam atmosphere. Fuel, 2020, 263, 116763.	6.4	24
76	Preparation of bimetallic catalysts Ni-Co and Ni-Fe supported on activated carbon for methane decomposition. Carbon Resources Conversion, 2020, 3, 190-197.	5.9	24
77	Effect of composition in coal liquefaction residue on catalytic activity of the resultant carbon for methane decomposition. Fuel, 2012, 96, 462-468.	6.4	23
78	Interaction between Hydrogen-Donor and Nondonor Solvents in Direct Liquefaction of Bulianta Coal. Energy & Fuels, 2016, 30, 10260-10267.	5.1	23
79	Novel insight into pyrolysis behaviors of lignin using in-situ pyrolysis-double ionization time-of-flight mass spectrometry combined with electron paramagnetic resonance spectroscopy. Bioresource Technology, 2020, 312, 123555.	9.6	23
80	Co-production of hydrogen and fibrous carbons by methane decomposition using K 2 CO 3 /carbon hybrid as the catalyst. International Journal of Hydrogen Energy, 2017, 42, 11047-11052.	7.1	22
81	Online analysis of initial volatile products of Shenhua coal and its macerals with pyrolysis vacuum ultraviolet photoionization mass spectrometry. Fuel Processing Technology, 2017, 163, 67-74.	7.2	22
82	Structural Features and Pyrolysis Behaviors of Extracts from Microwave-Assisted Extraction of a Low-Rank Coal with Different Solvents. Energy & Fuels, 2019, 33, 106-114.	5.1	22
83	Integrated Process of Coal Pyrolysis with CO ₂ Reforming of Methane by Dielectric Barrier Discharge Plasma. Energy & Fuels, 2011, 25, 4036-4042.	5.1	21
84	Preparation of mesoporous activated carbons from coal liquefaction residue for methane decomposition. Journal of Natural Gas Chemistry, 2012, 21, 759-766.	1.8	21
85	Co-pyrolysis of Baiyinhua lignite and pine in an infrared-heated fixed bed to improve tar yield. Fuel, 2020, 272, 117739.	6.4	21
86	Synthesis of hierarchical ZSM-5 by cetyltrimethylammonium bromide assisted self-assembly of zeolite seeds and its catalytic performances. Reaction Kinetics, Mechanisms and Catalysis, 2014, 113, 575-584.	1.7	20
87	Enhanced production of light tar from integrated process of in-situ catalytic upgrading lignite tar and methane dry reforming over Ni/mesoporous Y. Fuel, 2020, 279, 118533.	6.4	20
88	Highly Dispersed Rh/NbO _{<i>x</i>} Invoking High Catalytic Performances for the Valorization of Lignin Monophenols and Lignin Oil into Aromatics. ACS Sustainable Chemistry and Engineering, 2021, 9, 3529-3541.	6.7	20
89	Insights into effect of Ca(OH)2 on pyrolysis behaviors and products distribution of Hongshaquan coal. Fuel, 2022, 307, 121791.	6.4	20
90	Effects of the Catalyst and Reaction Conditions on the Integrated Process of Coal Pyrolysis with CO ₂ Reforming of Methane ^{â€} . Energy & Fuels, 2009, 23, 4782-4786.	5.1	19

#	Article	IF	CITATIONS
91	Pyrolysis behavior of low-density polyethylene over HZSM-5 via rapid infrared heating. Science of the Total Environment, 2022, 806, 151287.	8.0	19
92	Catalytic Liquefaction of Coal with Highly Dispersed Fe2S3 Impregnated in-Situ. Energy & Fuels, 2001, 15, 830-834.	5.1	18
93	Integrated process of coal tar upgrading and in-situ reduction of Fe2O3. Fuel Processing Technology, 2019, 191, 20-28.	7.2	18
94	Insight into synergistic effect of co-pyrolysis of low-rank coal and waste polyethylene with or without additives using rapid infrared heating. Journal of the Energy Institute, 2022, 102, 384-394.	5.3	18
95	Methylation of 2-Methylnaphthalene with Methanol to 2,6-Dimethylnaphthalene over ZSM-5 Modified by Zr and Si. Industrial & Engineering Chemistry Research, 2006, 45, 3531-3536.	3.7	17
96	Integrated process of coal pyrolysis with catalytic reforming of simulated coal gas for improving tar yield. Fuel, 2019, 255, 115797.	6.4	17
97	Quantitative characterization of coal structure by high-resolution CP/MAS 13C solid-state NMR spectroscopy. Proceedings of the Combustion Institute, 2021, 38, 4161-4170.	3.9	17
98	Insight into co-pyrolysis interactions of Pingshuo coal and high-density polyethylene via in-situ Py-TOF-MS and EPR. Fuel, 2021, 303, 121199.	6.4	17
99	Integrated process of coal pyrolysis with CO2 reforming of methane by spark discharge plasma. Journal of Analytical and Applied Pyrolysis, 2017, 126, 194-200.	5.5	16
100	Model for the Evolution of Pore Structure in a Lignite Particle during Pyrolysis. 2. Influence of Cross-Linking Reactions, Molten Metaplast, and Molten Ash on Particle Surface Area. Energy & Fuels, 2017, 31, 8036-8044.	5.1	16
101	Beyond Solution-Based Protocols: MOF Membrane Synthesis in Supercritical Environments for an Elegant Sustainability Performance Balance. , 2020, 2, 1142-1147.		16
102	In-situ catalytic cracking of coal pyrolysis tar coupled with steam reforming of ethane over carbon based catalyst. Fuel Processing Technology, 2020, 209, 106551.	7.2	16
103	In-situ catalytic upgrading of coal pyrolysis volatiles over red mud-supported nickel catalysts. Fuel, 2022, 324, 124742.	6.4	16
104	Xilinguole lignite pyrolysis under methane with or without Ni/Al2O3 as catalyst. Fuel Processing Technology, 2015, 136, 112-117.	7.2	15
105	Co-production of hydrogen-rich gas and porous carbon by partial gasification of coal char. Chemical Papers, 2018, 72, 273-287.	2.2	15
106	Integrated Process of Coal Pyrolysis with Steam Reforming of Ethane for Improving the Tar Yield. Energy & Fuels, 2018, 32, 12268-12276.	5.1	15
107	Integrated coal pyrolysis with steam reforming of propane to improve tar yield. Journal of Analytical and Applied Pyrolysis, 2020, 147, 104805.	5.5	15
108	Integrated coal pyrolysis with dry reforming of low carbon alkane over Ni/La2O3 to improve tar yield. Fuel, 2020, 266, 117092.	6.4	15

#	Article	IF	CITATIONS
109	Removal of elemental mercury in flue gas by Cu-Fe modified magnetosphere from coal combustion fly ash. Fuel, 2020, 271, 117668.	6.4	15
110	Novel detection of primary and secondary volatiles from cedar pyrolysis using in-situ pyrolysis double ionization time-of-flight mass spectrometry. Chemical Engineering Science, 2021, 236, 116545.	3.8	15
111	Co-pyrolysis behaviors of low-rank coal and polystyrene with in-situ pyrolysis time-of-flight mass spectrometry. Fuel, 2021, 286, 119461.	6.4	14
112	CO2 reforming of methane over activated carbon-Ni/MgO-Al2O3 composite catalysts for syngas production. Fuel Processing Technology, 2021, 211, 106595.	7.2	14
113	Experimental and Theoretical Investigation on Three α,ï‰-Diarylalkane Pyrolysis. Energy & Fuels, 2014, 28, 6905-6910.	5.1	13
114	Effects of Vitrinite in Low-Rank Coal on the Structure and Combustion Reactivity of Pyrolysis Chars. ACS Omega, 2020, 5, 17314-17323.	3.5	12
115	Pyrolysis behaviors of model compounds with representative oxygen-containing functional groups in coal over calcium. Fuel, 2022, 310, 122247.	6.4	12
116	Oxidative Catalytic Cracking and Reforming of Coal Pyrolysis Volatiles over NiO. Energy & Fuels, 2020, 34, 6928-6937.	5.1	11
117	Synthesis and modification of zeolite NaA adsorbents for separation of hydrogen and methane. Asia-Pacific Journal of Chemical Engineering, 2009, 4, 666-671.	1.5	10
118	Modified CPD Model for Coal Devolatilization at Underground Coal Thermal Treatment Conditions. Energy & Fuels, 2019, 33, 2981-2993.	5.1	10
119	Pyrolysis behaviors of coal-related model compounds catalyzed by pyrite. Fuel, 2020, 262, 116526.	6.4	10
120	Mechanism of methane decomposition with hydrogen addition over activated carbon via in-situ pyrolysis-electron impact ionization time-of-flight mass spectrometry. Fuel, 2020, 263, 116734.	6.4	10
121	Hydrogenation of naphthalene on nickel phosphide supported on silica. Asia-Pacific Journal of Chemical Engineering, 2009, 4, 574-580.	1.5	9
122	Methane decomposition with some CO2 as co-feed: Co-production of syngas and carbon fibers/microspheres by using a hybrid of K2CO3 and coal char. International Journal of Hydrogen Energy, 2018, 43, 6066-6075.	7.1	9
123	Integrated process of coal pyrolysis with dry reforming of low carbon alkane over Ni/La2O3-ZrO2 with different La/Zr ratio. Fuel, 2021, 292, 120412.	6.4	9
124	Effect of red mud-based additives on the formation characteristics of tar and gas produced during coal pyrolysis. Journal of the Energy Institute, 2022, 104, 1-11.	5.3	9
125	Adsorption separation performance of H2/CH4 on ETS-4 by concentration pulse chromatography. Journal of Energy Chemistry, 2014, 23, 213-220.	12.9	8
126	Effect of hydrogen addition on formation of hydrogen and carbon from methane decomposition over Ni/Al ₂ O ₃ . Canadian Journal of Chemical Engineering, 2020, 98, 536-543.	1.7	8

#	Article	IF	CITATIONS
127	Modeling the influence of changes in aliphatic structure on char surface area during coal pyrolysis. AICHE Journal, 2020, 66, e16834.	3.6	8
128	ZIF-derived hierarchical pore carbons as high-performance catalyst for methane decomposition. Journal of the Energy Institute, 2022, 100, 197-205.	5.3	8
129	Steam catalytic cracking of coal tar over ironâ€containing mixed metal oxides. Canadian Journal of Chemical Engineering, 2019, 97, 702-708.	1.7	7
130	Enhanced co-pyrolysis synergies between cedar and Naomaohu coal volatiles for tar production. Journal of Analytical and Applied Pyrolysis, 2021, 160, 105355.	5.5	7
131	Integrated process of coal pyrolysis and CO ₂ reforming of methane with and without using dielectric barrier discharge plasma. Energy Sources, Part A: Recovery, Utilization and Environmental Effects, 2016, 38, 613-620.	2.3	6
132	Upgrading of Heavy Oil with Chemical Looping Partial Oxidation over M ²⁺ Doped Fe ₂ O ₃ . Energy & Fuels, 2019, 33, 257-265.	5.1	6
133	In‣itu Upgrading of Coal Pyrolysis Tar with Steam Catalytic Cracking over Ni/Al ₂ O ₃ Catalysts. ChemistrySelect, 2020, 5, 4905-4912.	1.5	6
134	Modeling char surface area evolution during coal pyrolysis: Evolving characteristics with coal rank. Journal of Analytical and Applied Pyrolysis, 2021, 156, 105110.	5.5	6
135	Maximizing production of high-quality tar from catalytic upgrading of lignite pyrolysis volatiles over Ni-xCe/Y under CH4/CO2 atmosphere. Fuel, 2021, 297, 120767.	6.4	6
136	Insight to pyrolysis behavior of three aromatic ethers by pyrolysis coupled with single-photon ionization molecular-beam mass spectrometry. Fuel, 2021, 298, 120821.	6.4	6
137	Pyrolysis behaviors and product distributions of coal flotation sample separated by float and sink test. Fuel, 2022, 312, 122923.	6.4	6
138	Modeling char surface area evolution during coal pyrolysis: Effect of swelling and gasification at high pressures. Proceedings of the Combustion Institute, 2021, 38, 4151-4159.	3.9	5
139	Catalytic upgrading of ex-situ heavy coal tar over modified activated carbon. Fuel, 2022, 312, 122912.	6.4	5
140	Novel insight into the mechanism of coal hydropyrolysis using deuterium tracer method. Fuel, 2022, 321, 124109.	6.4	5
141	Study on pyrolysis behavior of long-chain n-alkanes with photoionization molecular-beam mass spectrometer. Journal of Analytical and Applied Pyrolysis, 2021, 159, 105324.	5.5	4
142	Process parameter optimization for integrated process of coal pyrolysis with dry reforming of low carbon alkane over Ni/La2O3–ZrO2. Journal of the Energy Institute, 2022, 102, 54-59.	5.3	4
143	Evaluation of coking coal by a modified fluorescence alteration of multiple macerals technique. Fuel, 2021, 291, 120138.	6.4	3
144	Insights into a Low-Rank Naomaohu Coal Structural Information by Multistage Fractions Coupled with LIAD-VUVPI-TOFMS. ACS Omega, 2022, 7, 6935-6943.	3.5	3

#	Article	IF	CITATIONS
145	Preparation of Ce–Mn/Fe ₂ O ₃ Catalysts for Steam Catalytic Cracking of Coal Tar. ChemistrySelect, 2018, 3, 12537-12543.	1.5	2
146	Catalytic performance of modified kaolinite in pyrolysis of benzyl phenyl ether: A model compound of low rank coal. Journal of the Energy Institute, 2020, 93, 2314-2324.	5.3	2
147	Modeling char surface area during coal pyrolysis: Validation of relationship between pore structure and polymer network. AICHE Journal, 2022, 68, .	3.6	2
148	Tuning the Acidity of Pt/ CNTs Catalysts for Hydrodeoxygenation of Diphenyl Ether. Journal of Visualized Experiments, 2019, , .	0.3	0
149	CO 2 Reforming of Methane over Feâ€Modified Niâ€Based Catalyst for Syngas Production. Energy Technology, 2020, 8, 1900231.	3.8	0
150	In-situ detection of initial products from lignite pyrolysis over modified Y-type zeolites by pyrolysis photoionization time-of-flight mass spectrometry. Chemical Engineering Science: X, 2020, 8, 100081.	1.5	0